

Biological Sciences: Genetics

**Extinct New Zealand megafauna were not in decline before human colonization**

Morten E. Allentoft<sup>1,2,3\*</sup>, Rasmus Heller<sup>4,5</sup>, Charlotte L. Oskam<sup>2</sup>, Eline D. Lorenzen<sup>6,1</sup>, Marie L. Hale<sup>3</sup>, M. Thomas P. Gilbert<sup>1</sup>, Chris Jacomb<sup>7</sup>, Richard N. Holdaway<sup>3,8</sup>, Michael Bunce<sup>2,9\*</sup>

- 1) Centre for GeoGenetics, Natural History Museum, University of Copenhagen, Øster Voldgade 5-7, 1350 Copenhagen K, Denmark.
- 2) Ancient DNA Laboratory, School of Veterinary and Life Sciences, Murdoch University, 90 South Street, Perth, Western Australia 6150, Australia.
- 3) School of Biological Sciences, University of Canterbury, Private Bag 4800, Christchurch 8140, New Zealand.
- 4) Department of Biology, University of Copenhagen, Universitetsparken 15, DK-2100 Copenhagen Ø, Denmark.
- 5) Instituto Gulbenkian de Ciência, Rua da Quinta Grande, 6 P-2780-156 Oeiras Portugal.
- 6) Department of Integrative Biology, University of California, Berkeley, California 94720, USA.
- 7) Southern Pacific Archaeological Research, Department of Anthropology and Archaeology, University of Otago, P.O. Box 56, Dunedin 9054, New Zealand.
- 8) Palaecol Research Ltd, 167 Springs Road, Hornby, Christchurch 8042, New Zealand.
- 9) Trace and Environmental DNA laboratory, Department of Environment and Agriculture, Curtin University, Perth, Western Australia, 6845, Australia

\* Correspondence:

Morten E. Allentoft

Centre for GeoGenetics, Natural History Museum of Denmark, University of Copenhagen, Øster Voldgade 5-7, 1350 Copenhagen K, Denmark.

morten.allentoft@gmail.com

+45 29824634

Michael Bunce

Trace and Environmental DNA laboratory, Department of Environment and Agriculture, Curtin University, Perth, Western Australia, 6845, Australia

michael.bunce@curtin.edu.au

+61 406998025

## **Abstract**

The extinction of New Zealand's moa (Aves: Dinornithiformes) followed the arrival of humans in the late 13th century and was the final event of the prehistoric late Quaternary megafauna extinctions. Determining the state of the moa populations in the pre-extinction period is fundamental to understanding the causes of the event. We sampled 281 moa individuals and combined radiocarbon dating with ancient DNA analyses to help resolve the extinction debate and gain new insights into moa biology. The samples, predominantly from the 4,000 years preceding the extinction, represent four sympatric moa species excavated from five adjacent fossil deposits. We characterised the moa assemblage using mitochondrial DNA and nuclear microsatellite markers developed specifically for moa. Although genetic diversity differed significantly among the four species, we find that the millennia preceding the extinction were characterised by a remarkable degree of genetic stability in all taxa, with no loss of heterozygosity and no shifts in allele frequencies over time. The extinction event itself was too rapid to be manifested in the moa gene pools. Contradicting previous claims of a decline in moa before Polynesian settlement in New Zealand, our findings indicate that the populations were large and stable before suddenly disappearing. This interpretation is supported by Approximate Bayesian Computation (ABC) analyses. Our analyses consolidate the disappearance of moa as the most rapid, human-facilitated megafauna extinction documented to date.

## **Significance statement**

In New Zealand, nine species of moa (large, wingless ratite birds) went extinct shortly after Polynesian settlement. In this study, we characterise the gene pools of four moa species during the final 4,000 years of their existence and gain new insights into moa biology and their population sizes. Our analyses show that moa populations were large and viable prior to human arrival in New Zealand and their demise therefore represents a striking example of human overexploitation of megafauna.

/body/

## **Introduction**

The causes of Late Quaternary megafauna extinctions continue to be debated (e.g., 1, 2, 3). Climate has been invoked as a major factor driving demographic shifts over evolutionary timescales but it is undeniable that most recent megafauna extinctions

occurred in the presence of humans. However, the role of humans in the extinction process differ among continents and the species studied (4) and it has proven difficult to evidence a direct causative link between anthropogenic activity and megafauna loss.

Ancient DNA research has contributed significantly to the extinction debate. DNA extracted from fossil material spanning thousands of years can yield insights into the demographic histories of extirpated populations and extinct species in the period leading up to their loss (5-7). However, most efforts have involved continental-scale data where the large geographic distances are hampering fine-scale inferences, limiting our ability to determine the causative agents of discrete demographic events. In contrast, island extinctions offer analytical advantages not afforded by studies of widely distributed species. In island endemics, the absence of gene flow from mainland populations allows us to disregard the spatial dimension in the genetic analyses and focus on extinction dynamics through time.

New Zealand is central to the megafauna extinction debate. It was the last major landmass to be colonized by humans and harboured a diverse assemblage of avian megafauna (8-10). Among them were nine species of moa (11): large, wingless ratite birds ranging in size from the ~12 kg North Island morph of *Euryapteryx curtus* to the ~250 kg females of the two *Dinornis* species (8). Moa inhabited a variety of habitats across the New Zealand archipelago until their extinction shortly after the arrival of Polynesian settlers, estimated around the late 13th century (8-10, 12). The abundance of well-preserved archaeological sites containing evidence of large-scale exploitation of moa (e.g., 13) brings the controversy of the role of humans in the extinction event into sharp focus.

Early claims of environmental changes or poor adaptive abilities of moa as causes for the extinction (reviewed in 8) have now been largely replaced by the view that direct or indirect human impacts, including hunting, fires and the introduction of exotic species, were the primary drivers (14-18). Ecological modelling suggests that such human-mediated extinction could have happened within 100 years of Polynesian colonization (10). In contrast, it has been argued based on limited mitochondrial DNA (mtDNA) data that moa populations had already collapsed before human arrival, as a

consequence of volcanic eruptions or diseases, suggesting that humans were just one of several additive factors responsible for the extinction (19).

To address this issue, we investigated the demographic trajectories of four sympatric moa species in the four millennia leading up to their extinction. We genotyped 281 individuals of *Dinornis robustus* (Dinornithidae) *Euryapteryx curtus*, *Pachyornis elephantopus*, and *Emeus crassus* (all Emeidae) using mtDNA and six nuclear microsatellite markers developed specifically for moa (20, 21). Moa were recovered from five fossil sites within a 10 km radius in North Canterbury on New Zealand's South Island (Figure 1). Through a series of genetic analyses, we have gained new insights into moa palaeobiology, population sizes and reproductive success, and have specifically addressed whether moa populations were in decline prior to Polynesian settlement of New Zealand.

## Results

### *Summary statistics*

The 217 radiocarbon-dated individuals covered a calibrated chronology from 12,966 BP to 602 BP (Table 1), although only 13 samples were older than 4,000 years BP (see individual sample ages in Dataset S1). We successfully amplified mtDNA sequences from 281 of 290 samples and retrieved reliable (20) microsatellite genotypes from 188 of the 217 radiocarbon-dated individuals.

Of 24 taxon-locus combinations, only two significant deviations from Hardy-Weinberg proportions were observed ( $\alpha = 0.05$ ) and only one after Bonferroni correction (Table S4). No tests for linkage disequilibrium among loci were significant ( $P > 0.07$ ) except for one instance in *P. elephantopus* (Moa\_MS2/Moa\_MA1;  $P = 0.0005$ ). The linkage could have resulted from a 106 bp homozygous profile in the Moa\_MS2 locus, which was accompanied by a 90 bp homozygous profile in the Moa\_MA1 locus in five individuals. This was probably an effect of the heterochronous data. Using established criteria (20), we did not find evidence of scoring bias from null alleles, allelic dropout, or stuttering in any of the data sets.

The four species differed in their levels of genetic diversity in both the mtDNA and microsatellite data (Figure 3, Table 2). Differences are visualised in the mtDNA haplotype networks (Figure 2), where the *E. crassus* gene pool is largely dominated by two haplotypes separated by a single mutation. Haplotype networks for *P. elephantopus* and *E. curtus* are provided in Figure S1.

The microsatellite markers were developed specifically for *D. robustus* (20, 21), and we therefore cannot eliminate ascertainment bias as being responsible for the lower levels of genetic diversity observed in the other species. However, the congruence between the relative diversity levels of the mtDNA and microsatellite data supports the validity of our data (Table 2). Also, ascertainment cannot explain the much lower genetic diversity in *E. crassus* in comparison to that in the other emeids (*E. curtus* and *P. elephantopus*); these three species are phylogenetically equidistant from *D. robustus* (11).

#### *Genetic structuring*

We find strong genetic differentiation among the four moa species (Figure S2). Only one of the 188 individuals with microsatellite profiles was assigned to the wrong species. Morphologically this tibiotarsus (AV8470 from Pyramid Valley) could only be a female *D. robustus* and the individual exhibited a rare combination of alleles for this species. We find no temporal genetic structuring within species, even when manipulating datasets to comprise only the ten oldest and ten youngest individuals for each species (Figure S2). This was supported by a lack of isolation-by-time using the Mantel test ( $P$ -values ranging from 0.24 to 0.48) and small insignificant  $F_{ST}$  values across time bins. In *D. robustus*, < 2.8% of the genetic variation was explained by temporal differentiation, and no pairwise  $F_{ST}$  values were significant (Table S5).

#### *Demographic history*

The Bayesian skyline plots of the three emeid species (*P. elephantopus*, *E. curtus*, *E. crassus*) displayed flat lines with large highest posterior densities (HPDs), likely reflecting a lack of power in the data to model a reliable genealogy, as has been reported for other ancient DNA megafauna data(22). We find support for a modest population expansion in *D. robustus* prior to human settlement of New Zealand. Despite the relatively large HPDs in the skyline plot, we find an increase in

population size  $c. 13,000$  BP (Figure 3, Table S1), although we were unable to reject the constant population size model as an alternative fit for the data. This increase was supported by the *free mode* of demographic change, which always yielded a posterior distribution with positive values for growth rate. Also, an *expand* model proved superior to a *decline* model, which consistently yielded *-infinity* likelihood values (Table S1).

The results from BEAST were supported by ABC analyses, which encompassed both mtDNA and microsatellite data. Under the *free model* approach, the modal value for the demographic change parameter ( $N_{anc}/N_{cur}$ ) was 0.9 (90% HPD interval 0.26–25.84), indicating that the population was unlikely to have changed dramatically in the period 31,700–100 years before the youngest sample (Table 3). The time of onset of demographic change had a wide posterior distribution (Table 3) as expected if the population size was constant, or only changed little. The population size at the time of human arrival was estimated to 9,200 individuals, but also with wide HPDs (Table 3). In the *model selection* approach we calculated a Bayes factor of 5.25 in favor of the *expand* model over the *decline* model. We observed good posterior coverage and high information content of the summary statistics, making us confident that the ABC analyses were informative with regards to model choice and parameter estimation (Table S3).

Despite allowing the effective population size of the mtDNA ( $N_{emt}$ ) remain independent of the autosomal (microsatellite) effective size ( $N_{ems}$ ) so as to assess whether there was support for an unequal reproductive contribution of the two sexes,  $N_{emt}$  remained close to the theoretically expected value of  $N_{ems}/4$  (posterior mode of  $N_{emt} = 3200$ ; posterior mode of  $N_{ems} = 15,800$ ). Hence we fixed  $N_{emt}$  to a quarter of  $N_{ems}$  in all reported simulations.

## **Discussion**

### *No pre-colonization decline in moa*

Our genetic data have provided a unique source of information regarding community-level megafauna population dynamics preceding the extinction event. We applied a range of methods to analyse mtDNA and microsatellite data and failed to detect any

evidence of moa decline, suggesting that the populations were large and viable throughout the Holocene until their sudden loss.

Temporal sampling is required to directly observe changes in genetic variability over time. To date, relatively few ancient DNA studies have included microsatellite data; those that do show that microsatellite analyses can be a powerful tool to detect temporal loss of genetic diversity and changes in allele frequencies (23-26). We observed no loss of genetic diversity in any of the four moa species (Figure 3). Moreover, we observed a star-like haplotype network in *Dinornis robustus*, which suggests an increase in population size (27, 28), although the signal may also reflect an artefact of analysing sequence data sampled across different points in time (29, 30). However, our detailed demographic analyses of *D. robustus*, using BEAST and ABC, take temporal sampling into account, and support a scenario of a slowly increasing population size during the Holocene.

All moa were sampled from within a 10 km radius, and we can therefore disregard geographic structuring patterns and focus exclusively on genetic patterns through time. Our observation of Hardy-Weinberg proportions and no linkage disequilibrium in the moa populations could be interpreted as random mating. However, these samples span several millennia and rather, the result reflects that the microsatellite allele frequencies remained roughly constant during the entire second half of the Holocene. This is also supported by absence of temporal genetic structuring and lack of isolation-by-time. Our results reflect very low levels of genetic drift, in agreement with a recent mtDNA analysis of the moa genus *Pachyornis* which also failed to detect significant demographic shifts during this period (31).

Despite comprehensive genetic analyses of four moa species, we found no genetic signatures of a hypothesized Holocene pre-human decline. The previous study describing this population collapse (19) may have been compromised by some questionable assumptions (discussed in 32). Rather, our results indicate that the *D. robustus* population increased slowly at the onset of the Holocene which seems reasonable from an ecological perspective. Moa were primarily forest and shrubland dwellers, with some entering herbfields and the subalpine zone (8, 33), and pollen records from the South Island reflect an establishment of post-glacial shrubland

14,000-10,000 years BP, followed by podocarp forest expansion around 13,600-7,500 years BP (34, 35).

#### *Population size of *Dinornis robustus**

Our data suggest that *D. robustus* had an effective population size ( $N_e$ ) of *c.* 9,200 individuals when Polyneisians reached New Zealand. Although the posterior distributions are wide, this is the modal value from the 'free-model' ABC analysis (Table 3) which encompass both mtDNA and nuclear microsatellite data and is without any directional restrictions on simulated growth rate. The conversion of effective population size to census population size ( $N_c$ ) is problematic, especially for extinct taxa with limited biological information, and no  $N_e:N_c$  ratios have been published for extant ratites. However, our best estimate of  $N_e:N_c$  ratio for *D. robustus* is 0.4 (see SI text). With an  $N_e$  of 9,200 we therefore estimate a census size of *c.* 25,000 *D. robustus* individuals which is the same order of magnitude as the 14,100 individuals estimated from ecological modelling (see SI text and Dataset S2, S3). Such a large population size of a heavy and slowly maturing species (36) suggests a larger, panmictic South Island population, rather than a local enclave isolated in North Canterbury. This suggests that *D. robustus* individuals could disperse over long distances and sustain population connectivity in a landscape fragmented by rivers, glaciers and mountain ranges. It seems reasonable to infer that for flightless birds, larger body size translates into higher dispersal rates, resulting in larger effective population sizes and higher levels of genetic diversity. This could also explain why the smallest species of the region (*E. crassus*) had the lowest observed genetic diversity (Table 2).

The fossil record suggests that moa had skewed sex ratios with an excess of females (8, 37). If the sexes did not contribute evenly to the effective population size, we would expect a deviation from a 1:4 ratio between mtDNA and microsatellite (autosomal) effective population sizes. Indeed, we observe a 1:4 ratio in the ABC analysis of *D. robustus*, suggesting that putative skewed sex ratios did not cause differential reproductive success between the sexes. Our result could indicate mating competition among females and accordance with the observation of pronounced reverse sexual size-dimorphism (38, 39) and hypotheses of female territoriality (37) in moa.



### *Genetic diversity in the moa community*

We found differing levels of genetic diversity in the four moa species, although each remained constant through time (Figure 3, Table 2). In the four millennia preceding extinction, we found only half the genetic diversity in *Emeus crassus* compared with the three other moa species, suggesting either a smaller population size or a previous demographic bottleneck. Unlike *Euryapteryx curtus* and *Pachyornis elephantopus*, *E. crassus* was not present in the wetter western and northwestern South Island during the Pleistocene (40); the more limited distribution likely resulted in smaller population sizes. If a bottleneck was the cause of lower levels of genetic diversity in *E. crassus*, it could reflect population isolation in a habitat refugium during the Otiran glaciation, c. 74,000-17,900 years BP (41), followed by re-colonisation of the Eastern lowlands including North Canterbury, when suitable habitat increased at the onset of the Holocene (e.g., 11). Despite markedly lower genetic diversity, *E. crassus* appears to have been thriving in the Eastern forests, where late Holocene fossils have been found in great abundance (42, 43).

### *Conclusion*

This study has highlighted the palaeobiological insights that can be gained from ancient population genetics beyond the traditional analyses of mtDNA. We profiled 281 individual moa of four species in the 4,000 years preceding their extinction by combining radiocarbon dating, mtDNA sequencing and nuclear microsatellite genotyping. We observed differing levels of genetic diversity between species in the Holocene moa community. For *D. robustus* we found an equal reproductive output between sexes, and estimated the population size and demography leading up to the extinction event. Interestingly, the moa extinction process did not leave any genetic traces in our data, very likely because it was too short for increased genetic drift to have an effect on the gene pools. Our results do not support a collapse in any of the moa populations in the millennia preceding Polynesian settlement of New Zealand (19). Rather, our detailed analysis of *D. robustus* indicated that this moa species increased in numbers during the Holocene. When humans arrived in New Zealand they encountered a large and perhaps still increasing *D. robustus* population with an estimated effective size of 9,200 individuals. From the archaeological record we know that moa were hunted intensively and that *D. robustus* disappeared along with eight

other moa species within just one or two centuries following human arrival (10). Taken together this points strongly towards human contact as the only factor responsible for the extinction.

## **Materials and methods**

### *Sampling, extraction, identification, and age*

A total of 290 moa fossils from five adjacent Holocene fossil deposits (Figure 1) was sampled according to established protocols (21, 44). To avoid including more than one sample from each individual, only left tibiotarsi were sampled, except for one right femur (AV 41188) that was not associated with any of the tibiotarsi (based on consideration of fossil site, bone size, and preservation). DNA extractions from 200 mg aliquots of bone powder were performed in a dedicated aDNA facility (Murdoch University, Perth, Australia) using a silica-column based method (21). Genetic sex-identifications were taken from previous work (37, 44) as were 158 of the 217 calibrated radiocarbon ages (45); the experimental procedures are detailed in these references. The dates presented in this study are median calibrated ages (years BP) using the SHCAL04 curve in OxCal v4.1 (Oxford Radiocarbon Accelerator Unit). An overview of the material is presented in Table 1, and individual data in Dataset S1.

### *PCR and authentication*

Two primer sets (185F/294R and 262F/441R) were used to amplify a 337-341 bp fragment (excluding primers) of the moa mtDNA control region (CR). This region has previously proven informative for assessing intra- and interspecific genetic differentiation in moa (11) and PCR conditions are described elsewhere (37, 38). PCR products were sequenced in both directions and samples with DNA sequences that continually yielded ambiguous base calls (nine of the 290 samples) were excluded from further analyses, yielding a total of 281 samples. Samples with mutations, appearing less than three times in the overall sequence alignments, were sequenced and observed at least twice from independent PCRs before being accepted.

Information on the six microsatellite loci and their PCR conditions are provided in previous work (20, 21). To overcome the challenges introduced by allelic dropout, we followed the strict guidelines set out previously (20). We restricted the microsatellite profiling to the 217 radiocarbon-dated individuals.

### *Summary statistics*

The mtDNA sequences were aligned in Geneious v. 4.8.3 (46), and imported into DNASP v. 5.10 (47) to calculate genetic diversity. Microsatellite genetic diversity was calculated in GenAlEx v.6.4 (48). Deviations from Hardy-Weinberg proportions were quantified as  $F_{IS}$ , (49), and significance was tested with the exact test in GENEPOP v.4.0.10 (50). Deviations from linkage equilibrium were also tested with GENEPOP. We used MICRO-CHECKER v.2.2.3 (51) to investigate the presence of null alleles and allelic dropout.

### *Genetic structure*

To visualize the genetic structure and diversity of the mtDNA sequences in each of the four species, we generated median-joining haplotype networks with NETWORK v. 4.5 (<http://www.fluxus-engineering.com>). We used STRUCTURE ver. 2.3.3 (52) on the microsatellite data to perform several analyses to detect genetic structuring within and among species (SI text). The fixation index ( $F_{ST}$ ) was used to quantify intraspecific genetic differentiation based on the microsatellite data. As all individuals were sampled within a radius of 10 km, geographic differentiation was not relevant to our study and we instead investigated genetic differentiation across time. Using the age of each sample, we constructed temporal groups by pooling individuals into 1000 calendar years.  $F_{ST}$  values between all pairs of groups were calculated (49), and the significance of the differentiation was assessed by a permutation test using FSTAT ver. 2.9.3 (53). A Mantel test is commonly applied to assess genetic isolation-by-distance but it should be equally suitable for detection of 'genetic isolation-by-time'. Based on microsatellite data, matrices of temporal and genetic distances between all pairs of individuals (within each species separately) were generated and tested for correlations using the Mantel test in GenAlEx ver. 6 (48). The temporal distances were recorded as the number of calendar years that separated two individuals. We assessed the  $P$ -value of each correlation with 1000 randomisations.

### *Demographic history*

We used two overall methods to estimate demographic history: BEAST and Approximate Bayesian Computation (ABC). We analyzed the 217 radiocarbon-dated mtDNA sequences in BEAST ver. 1.6.1 (54). JMODELTEST ver. 0.1.1 (55) and the Akaike Information Criterion (AIC) (56) was used to estimate the most likely

substitution model, favoring a HKY+I+G model for all four species. Prior values on parameters associated with this substitution model were estimated in JMODELTEST and incorporated in BEAST using wide prior distributions. We analysed each species data set using the Bayesian Skyline model which allows population sizes to fluctuate freely through time as governed by the data. *D. robustus* represented the largest of the data sets (most radiocarbon dates, Table 1), and is the species for which a Holocene decline has been claimed (19). We therefore analysed this species in more detail and tested an additional four demographic models (Table S1). These were (i) a *constant* population size model, and three different single-change-point models, assuming a constant population size replaced by an exponential change in population size. These models were (ii) a *free model*, allowing both exponential growth and decline, (iii) an *expand* model allowing only growth, as expected when more favourable moa habitat became available after the end of the most recent glaciation in New Zealand, 74,000-17,900 years BP (41), and (iv) a *decline* model, allowing only population decline, following the scenario suggested previously (19). Parameter details are provided in SI text and Table S1. BEAST output files were analysed in TRACER ver. 1.5 (57) after removing the first 10% of the trees as burn-in. The different models were compared with marginal likelihoods after 1000 bootstraps.

We used ABC simulations to further elucidate the demographic history of *D. robustus*. Comparable to the BEAST analyses, we used two different approaches: the *free model* approach under which the population size in the most recent phase of the demographic history was allowed to change by a factor of 100 (decline or expansion), and the *model selection* approach where we compared two discrete scenarios of historical population dynamics with declining or expanding population size (Table 3) and compared their respective fit to our observed data using 19 summary statistics (Table S2). See SI text for details on the ABC analyses.

### **Acknowledgements**

We acknowledge the Museum of New Zealand, Te Papa Tongarewa (A.J.D. Tennyson), Canterbury Museum (P. Scofield) and The American Museum of Natural History (C. Mehling). We thank Eske Willerslev, Malene Møhl, James Haile and Ross Barnett for assistance with the sequencing and sampling, and Jayne Houston, Emma McLay, Helen Hunt and Frances Brigg for technical assistance. Thanks to

Daniel Wegmann, Simon Ho, Christian Anderson, Alexei Drummond and Che Si Wu for advice on the analyses. We thank Giesen and Veldhuizen (Bell Hill Vineyard) and the Hodgen family (Pyramid Valley) for their support of our research. Funding was provided by the Marsden Fund of the Royal Society of New Zealand (contracts 06-PAL-001-EEB to Palaecol Research Ltd (RNH), and 09-UOO-164 to Otago University (CJ)). MEA and MB are funded by the European Research Council (Marie Curie Actions, Grant Agreement n. 300554), and the Australian Research Council (Future Fellowship FT0991741), respectively.

## References

1. Alroy J (2001) A Multispecies Overkill Simulation of the End-Pleistocene Megafaunal Mass Extinction. *Science* 292(5523):1893-1896.
2. Koch PL & Barnosky AD (2006) Late quaternary extinctions: State of the debate. *Annual Review of Ecology Evolution and Systematics* 37:215-250.
3. Stuart AJ, Kosintsev PA, Higham TFG, & Lister AM (2004) Pleistocene to Holocene extinction dynamics in giant deer and woolly mammoth. *Nature* 431(7009):684-689.
4. Lorenzen ED, *et al.* (2011) Species-specific responses of Late Quaternary megafauna to climate and humans. *Nature* 479(7373):359-364.
5. Shapiro B, *et al.* (2004) Rise and fall of the Beringian steppe bison. *Science* 306(5701):1561-1565.
6. Campos PF, *et al.* (2010) Ancient DNA analyses exclude humans as the driving force behind late Pleistocene musk ox (*Ovibos moschatus*) population dynamics. *Proceedings of the National Academy of Sciences*.
7. Palkopoulou E, *et al.* (2013) Holarctic genetic structure and range dynamics in the woolly mammoth. *Proceedings of the Royal Society B: Biological Sciences* 280(1770).
8. Worthy TH & Holdaway RN (2002) *The lost world of the Moa* (Canterbury University Press, Christchurch) p 718.
9. Anderson A (1989) Mechanics of Overkill in the Extinction of New-Zealand Moas. *Journal of Archaeological Science* 16(2):137-151.
10. Holdaway RN & Jacomb C (2000) Rapid extinction of the moas (Aves : Dinorinthiformes): Model, test, and implications. *Science* 287(5461):2250-2254.
11. Bunce M, *et al.* (2009) The evolutionary history of the extinct ratite moa and New Zealand Neogene paleogeography. *Proceedings of the National Academy of Sciences of the United States of America* 106(49):20646-20651.
12. Higham T, Anderson A, & Jacomb C (1999) Dating the first New Zealanders: The chronology of Wairau Bar. *Antiquity* 73(280):420-427.
13. Oskam CL, *et al.* (2011) Molecular and morphological analyses of avian eggshell excavated from a late thirteenth century earth oven. *Journal of Archaeological Science* In Press, Corrected Proof.
14. Anderson A (1989) *Prodigious Birds* (Cambridge University Press, Cambridge, England).

15. Holdaway RN (1989) New Zealand's pre-human avifauna and its vulnerability. *New Zealand Journal of Ecology* 12:11-25.
16. Holdaway RN (1996) Arrival of rats in New Zealand. *Nature* 384(6606):225-226.
17. McWethy DB, Whitlock C, Wilmshurst JM, McGlone MS, & Li X (2009) Rapid deforestation of South Island, New Zealand, by early Polynesian fires. *Holocene* 19(6):883-897.
18. Wilmshurst JM, Anderson AJ, Higham TFG, & Worthy TH (2008) Dating the late prehistoric dispersal of polynesians to New Zealand using the commensal Pacific rat. *Proceedings of the National Academy of Sciences of the United States of America* 105(22):7676-7680.
19. Gemmell NJ, Schwartz MK, & Robertson BC (2004) Moa were many. *Proceedings of the Royal Society of London Series B-Biological Sciences* 271:S430-S432.
20. Allentoft ME, *et al.* (2011) Profiling the dead: generating microsatellite data from fossil bones of extinct megafauna—protocols, problems, and prospects. *PLoS ONE* 6(1):e16670.
21. Allentoft ME, *et al.* (2009) Identification of microsatellites from an extinct moa species using high-throughput (454) sequence data. *Biotechniques* 46:195-200.
22. Bon C, *et al.* (2008) Deciphering the complete mitochondrial genome and phylogeny of the extinct cave bear in the Paleolithic painted cave of Chauvet. *Proceedings of the National Academy of Sciences* 105(45):17447-17452.
23. Whitehouse AM & Harley EH (2001) Post-bottleneck genetic diversity of elephant populations in South Africa, revealed using microsatellite analysis. *Molecular Ecology* 10(9):2139-2149.
24. Nyström V, *et al.* (2012) Microsatellite genotyping reveals end-Pleistocene decline in mammoth autosomal genetic variation. *Molecular Ecology* 21(14):3391-3402.
25. Shepherd LD, *et al.* (2005) Microevolution and mega-icebergs in the Antarctic. *Proceedings of the National Academy of Sciences of the United States of America* 102(46):16717-16722.
26. Harper GL, Maclean N, & Goulson D (2006) Analysis of museum specimens suggests extreme genetic drift in the adonis blue butterfly (*Polyommatus bellargus*). *Biological Journal of the Linnean Society* 88(3):447-452.
27. Rogers AR & Harpending H (1992) Population growth makes waves in the distribution of pairwise genetic differences. *Molecular Biology and Evolution* 9(3):552-569.
28. Slatkin M & Hudson RR (1991) Pairwise comparisons of mitochondrial DNA sequences in stable and exponentially growing populations. *Genetics* 129(2):555-562.
29. Debruyne R & Poinar HN (2009) Time Dependency of Molecular Rates in Ancient DNA Data Sets, A Sampling Artifact? *Systematic Biology* 58(3):348-359.
30. Depaulis F, Orlando L, & Hanni C (2009) Using Classical Population Genetics Tools with Heterochronous Data: Time Matters! *PLoS ONE* 4(5).
31. Rogaev EI, *et al.* (2006) Complete Mitochondrial Genome and Phylogeny of Pleistocene Mammoth. *PLoS Biol* 4(3):e73.
32. Allentoft ME & Rawlence NJ (2012) Moa's Ark or volant ghosts of Gondwana? Insights from nineteen years of ancient DNA research on the

- extinct moa (Aves: Dinornithiformes) of New Zealand. *Annals of Anatomy - Anatomischer Anzeiger* 194(1):36-51.
33. Wood JR, *et al.* (2013) Resolving lost herbivore community structure using coprolites of four sympatric moa species (Aves: Dinornithiformes). *Proceedings of the National Academy of Sciences of the United States of America* 110(42):16910-16915.
  34. Moar NT (2008) Late Quaternary Vegetation. *The Natural History of North Canterbury*, eds Winterbourn MJ, Knox GA, Burrows CJ, & Marsden ID (Canterbury University Press, Christchurch), pp 169-192.
  35. McGlone MS, Turney CSM, & Wilmshurst JM (2004) Late-glacial and Holocene vegetation and climatic history of the Cass basin, central south island, New Zealand. *Quaternary Research* 62(3):267-279.
  36. Turvey ST, Green OR, & Holdaway RN (2005) Cortical growth marks reveal extended juvenile development in New Zealand moa. *Nature* 435(7044):940-943.
  37. Allentoft ME, Bunce M, Scofield RP, Hale ML, & Holdaway RN (2010) Highly skewed sex ratios and biased fossil deposition of moa: ancient DNA provides new insight on New Zealand's extinct megafauna. *Quaternary Science Reviews* 29(5-6):753-762.
  38. Bunce M, *et al.* (2003) Extreme reversed sexual size dimorphism in the extinct New Zealand moa *Dinornis*. *Nature* 425(6954):172-175.
  39. Huynen L, Millar CD, Scofield RP, & Lambert DM (2003) Nuclear DNA sequences detect species limits in ancient moa. *Nature* 425(6954):175-178.
  40. Worthy TH & Holdaway RN (1993) Quaternary fossil faunas from caves in the Punakaiki area, West Coast, South Island, New Zealand. *Journal of the Royal Society of New Zealand* 23(3):147-254.
  41. Lorrey AM, *et al.* (2012) Palaeocirculation across New Zealand during the last glacial maximum at similar to 21 ka. *Quaternary Science Reviews* 36:189-213.
  42. Holdaway RN & Worthy TH (1997) A reappraisal of the late quaternary fossil vertebrates of Pyramid Valley Swamp, North Canterbury, New Zealand. *New Zealand Journal of Zoology* 24(1):69-121.
  43. Worthy TH & Holdaway RN (1996) Quaternary fossil faunas, overlapping taphonomies, and palaeofaunal reconstruction in north Canterbury, South Island, New Zealand. *Journal of the Royal Society of New Zealand* 26(3):275-361.
  44. Allentoft ME, *et al.* (2012) A molecular characterisation of a newly discovered megafaunal fossil site in North Canterbury, South Island, New Zealand. *Journal of the Royal Society of New Zealand* 42(4):241-256.
  45. Allentoft ME, *et al.* (2012) The half-life of DNA in bone: measuring decay kinetics in 158 dated fossils. *Proceedings of the Royal Society B: Biological Sciences* 279(1748):4724-4733.
  46. Drummond AJ, *et al.* (2010) Geneious ver. 5.1 (Available from <http://www.geneious.com>).
  47. Librado P & Rozas J (2009) DnaSP v5: a software for comprehensive analysis of DNA polymorphism data. *Bioinformatics* 25(11):1451-1452.
  48. Peakall R & Smouse PE (2006) GENALEX 6: genetic analysis in Excel. Population genetic software for teaching and research. *Molecular Ecology Notes* 6(1):288-295.
  49. Weir BS & Cockerham CC (1984) Estimating F-statistics for the analysis of population structure. *Evolution* 38(6):1358-1370.

50. Rousset F (2008) GENEPOP ' 007: a complete re-implementation of the GENEPOP software for Windows and Linux. *Molecular Ecology Resources* 8(1):103-106.
51. van Oosterhout C, Weetman D, & Hutchinson WF (2006) Estimation and adjustment of microsatellite null alleles in nonequilibrium populations. *Molecular Ecology Notes* 6(1):255-256.
52. Pritchard JK, Stephens M, & Donnelly P (2000) Inference of population structure using multilocus genotype data. *Genetics* 155(2):945-959.
53. Goudet J (2001) FSTAT, a program to estimate and test gene diversities and fixation indices (version 2.9.3). Available from: <http://www.unil.ch/izea/software/fstat>.
54. Drummond AJ & Rambaut A (2007) BEAST: Bayesian evolutionary analysis by sampling trees. *BMC Evolutionary Biology* 7(214).
55. Posada D (2008) jModelTest: Phylogenetic model averaging. *Molecular Biology and Evolution* 25(7):1253-1256.
56. Akaike H (1974) New look at statistical model identification. *Transactions on Automatic Control* 19(6):716-723.
57. Rambaut A & Drummond A (2007) Tracer (Available from <http://beast.bio.ed.ac.uk/Tracer>).
58. Rawlence NJ, *et al.* (2011) New palaeontological data from the excavation of the Late Glacial Glencrieff miring bone deposit, North Canterbury, South Island, New Zealand. *Journal of the Royal Society of New Zealand* 41(3):217-236.

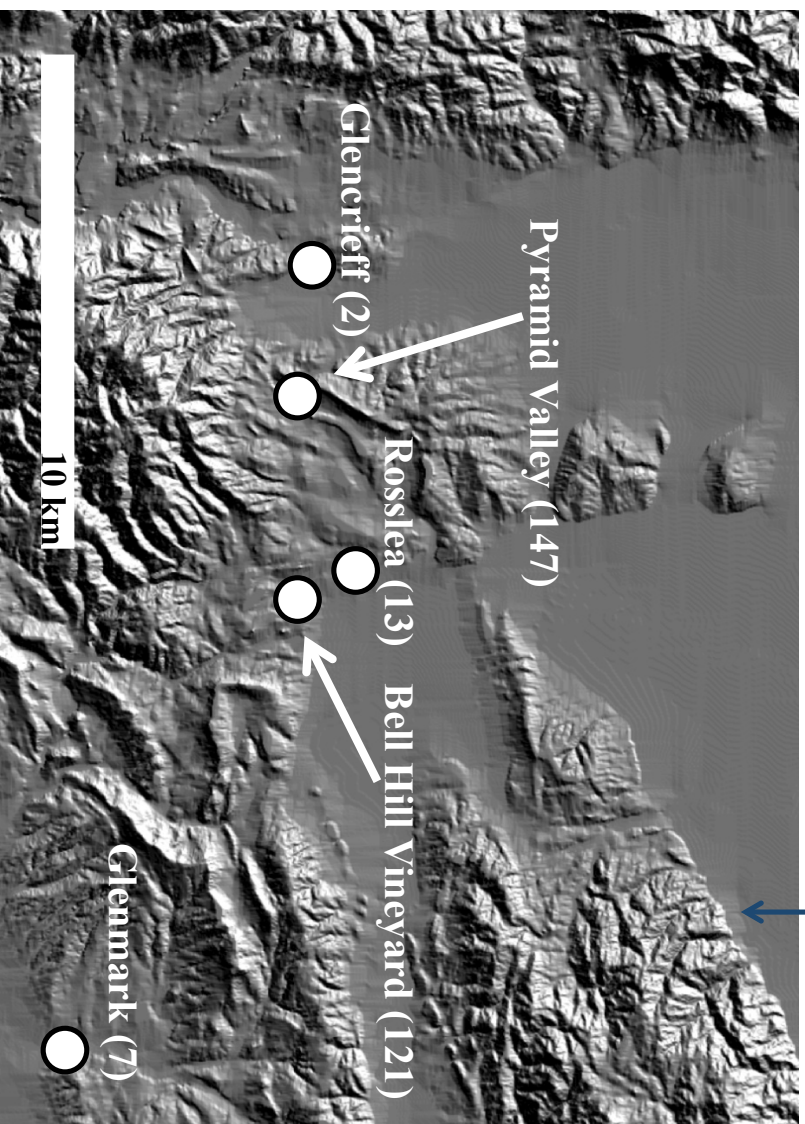
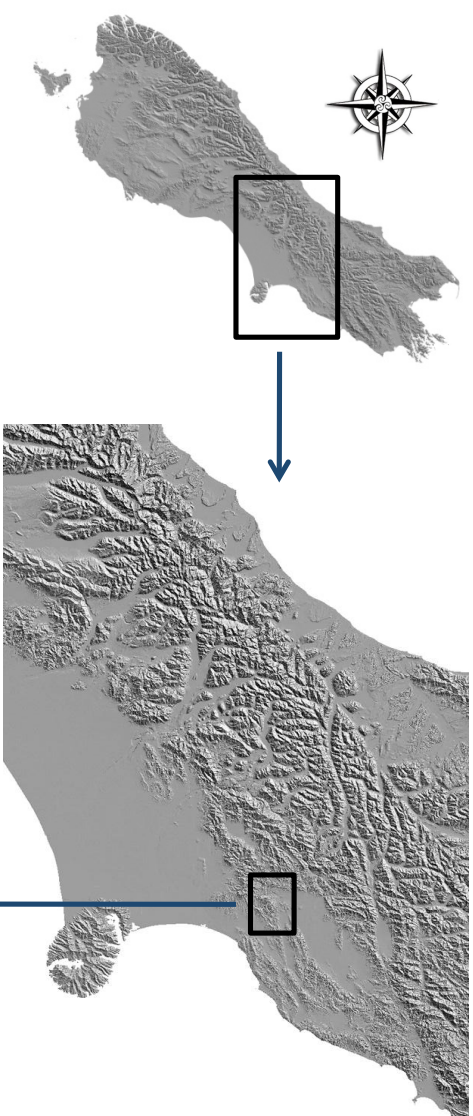
## Figure legends

**Figure 1:** Map of the study sites in North Canterbury, South Island, New Zealand. All sites represent well-described moa fossil assemblages, with geographical coordinates as follows: Pyramid Valley (42°58'22.0"S, 172°35'49.0"E) (42), Bell Hill Vineyard (42°58'19.36"S, 172°39'56.15"E) (37), Rosslea, (42°57'53.83"S, 172°39'22.39"E) (44), Glenmark (43°00'00.0"S, 172°46'50.0"E) (43), Glencrieff (42°58'07.45"S, 172°34'01.84"E) (58). Sample sizes are in parantheses.

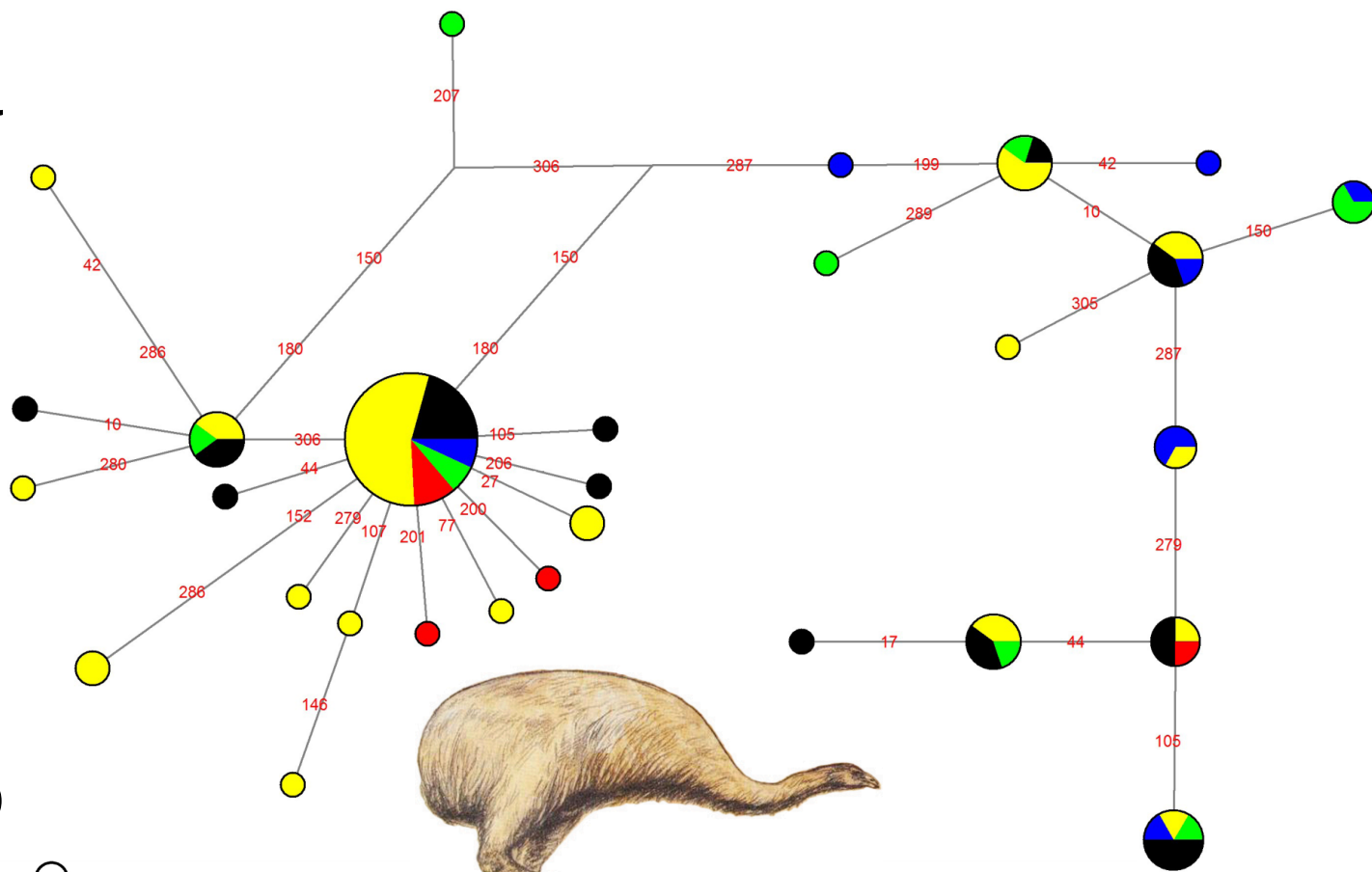
**Figure 2:** mtDNA haplotype networks of (a) *Dinornis robustus*,  $n = 87$  and (b) *Emeus crassus*,  $n = 81$ , based on 442 bp of mtDNA. The color composition of each haplotype is defined by the individual radiocarbon ages of the fossils. See Table 2 for summary statistics.



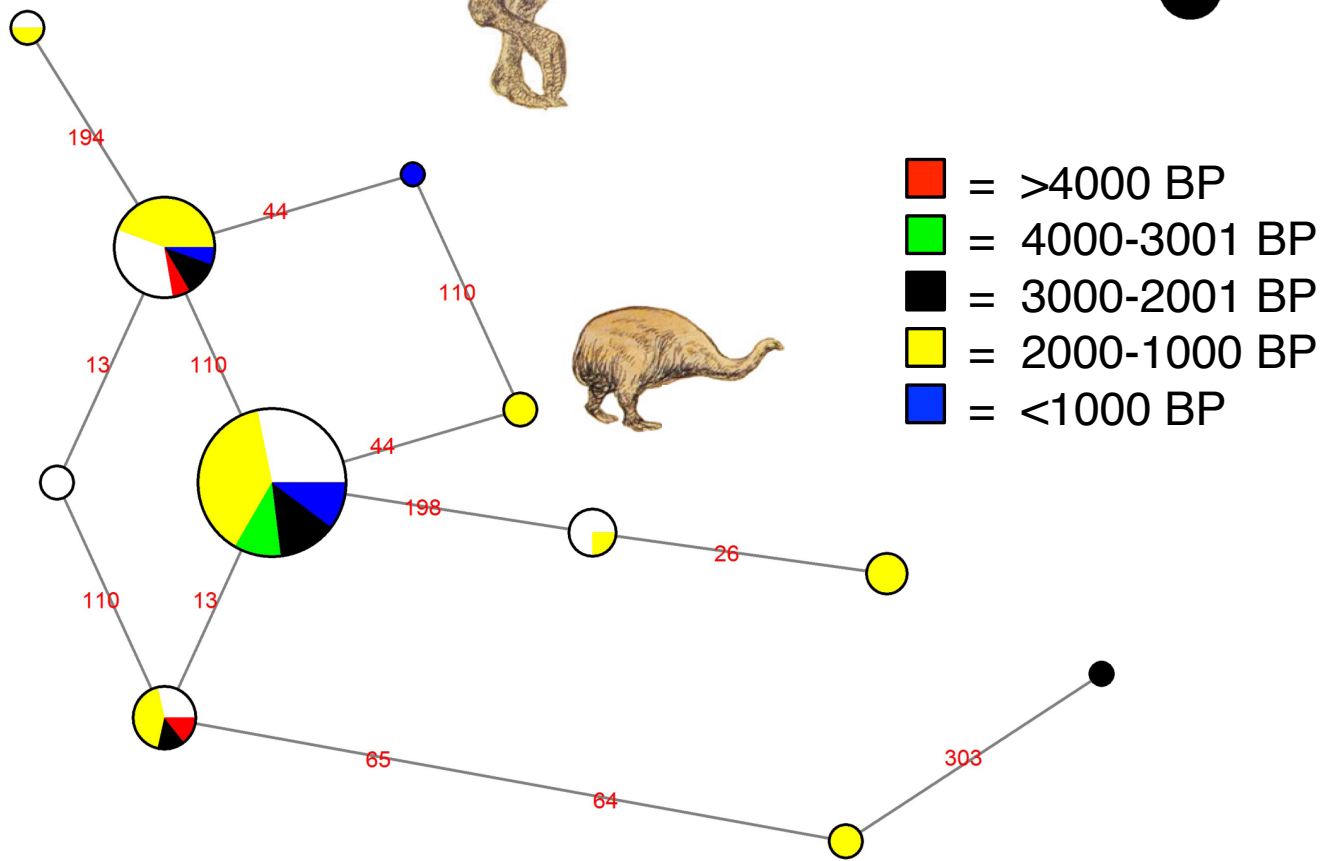
**Figure 3:** Demographic history and genetic diversity. a) Bayesian Skyline Plot for *D. robustus* ( $n = 87$ ), where y-axis depicts the effective female population size multiplied by generation time. Year *zero* corresponds to the age of the youngest sample at 602 BP. b) Expected heterozygosity ( $H_E$ ) for six microsatellite loci, measured across time in the four moa species ( $n = 188$ ). Data points represent the mean age and mean  $H_E$  (with standard error) of the moa individuals in 1000-year time bins.



a



b



- = >4000 BP
- = 4000-3001 BP
- = 3000-2001 BP
- = 2000-1000 BP
- = <1000 BP

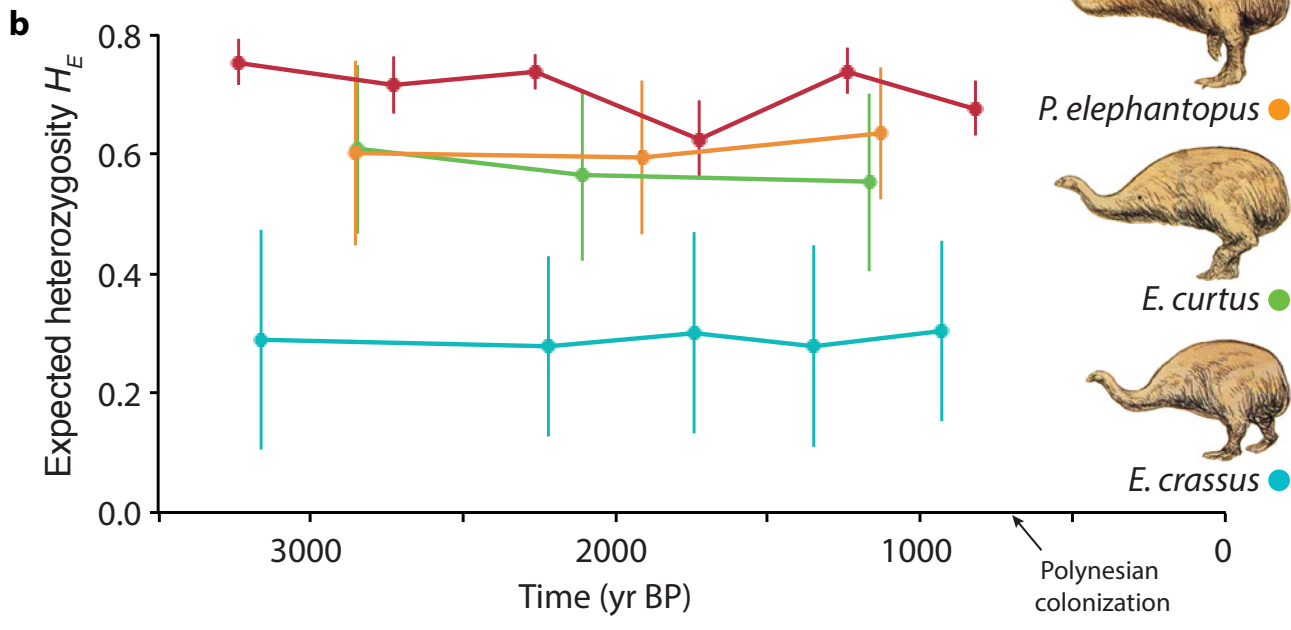
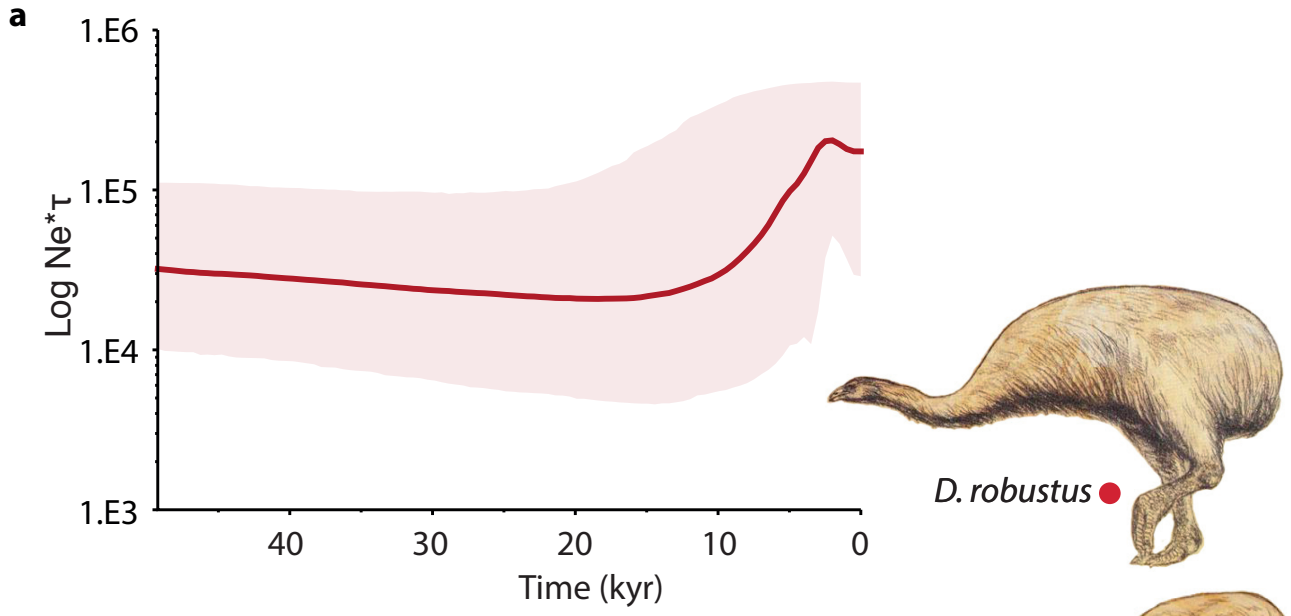


**Table 1:** Time span of calibrated radiocarbon ages for sites and species.

| Site               | Sampled | Dated | Age           |
|--------------------|---------|-------|---------------|
| Pyramid Valley     | 147     | 127   | 4136-602 BP   |
| Bell Hill Vineyard | 121     | 74    | 2876-851 BP   |
| Rosslea            | 13      | 8     | 7839-1482 BP  |
| Glenmark           | 7       | 6     | 5152-782 BP   |
| Glencrieff         | 2       | 2     | 12966-4837 BP |
| Total              | 290     | 217   | 12966-602 BP  |

| Taxon                  | Sampled | Dated | Age          |
|------------------------|---------|-------|--------------|
| <i>D. robustus</i>     | 89      | 88    | 12966-602 BP |
| <i>P. elephantopus</i> | 32      | 32    | 4067-853 BP  |
| <i>E. curtus</i>       | 84      | 40    | 5812-945 BP  |
| <i>E. crassus</i>      | 85      | 57    | 5791-874 BP  |
| Total                  | 290     | 217   | 12966-602 BP |

**Table 2:** Genetic diversity

| mtDNA                  |     |        |     |     |       |      |
|------------------------|-----|--------|-----|-----|-------|------|
| Taxon                  | $n$ | length | $h$ | $S$ | $\pi$ | $k$  |
| <i>D. robustus</i>     | 87  | 341 bp | 29  | 24  | 0.010 | 3.44 |
| <i>P. elephantopus</i> | 31  | 337 bp | 13  | 15  | 0.008 | 2.55 |
| <i>E. curtus</i>       | 82  | 338 bp | 16  | 15  | 0.007 | 2.29 |
| <i>E. crassus</i>      | 81  | 337 bp | 11  | 9   | 0.004 | 1.19 |

| Microsatellites        |     |       |       |       |       |          |
|------------------------|-----|-------|-------|-------|-------|----------|
| Taxon                  | $n$ | $N_A$ | $N_E$ | $H_O$ | $H_E$ | $F_{IS}$ |
| <i>D. robustus</i>     | 74  | 9.5   | 3.8   | 0.687 | 0.721 | 0.040    |
| <i>P. elephantopus</i> | 30  | 7.2   | 3.9   | 0.561 | 0.601 | 0.041    |
| <i>E. curtus</i>       | 29  | 8.7   | 4.6   | 0.600 | 0.570 | -0.079   |
| <i>E. crassus</i>      | 55  | 4.7   | 2.4   | 0.305 | 0.288 | -0.048   |

Intraspecific summary statistics for the four species.  $n$ , number of analysed individuals for mtDNA and nuclear microsatellite loci respectively; length of analysed DNA fragment excluding primers;  $h$ , observed number of haplotypes;  $S$ , number of segregating sites;  $\pi$ , nucleotide diversity;  $k$ , average number of nucleotide differences between two sequences;  $N_A$ , average number of observed alleles per locus;  $N_E$ , average number of effective alleles per locus;  $H_O$ , observed heterozygosity;  $H_E$ , expected heterozygosity;  $F_{IS}$ , fixation index.

**Table 3:** ABC analysis

| Priors                          | $N_{cur}$            | $N_{anc}/N_{cur}$ | $T$                | $\mu$                  | $p$              | Marginal density |
|---------------------------------|----------------------|-------------------|--------------------|------------------------|------------------|------------------|
| <i>Free model</i>               | 500–50,000           | 0.01–100          | 100–31,700         | $10^{-3}$ – $10^{-5}$  | 0.4–0.9          | 0.31             |
| <i>Model selection: decline</i> | 500–50,000           | 1–100             | 100–31,700         | $10^{-3}$ – $10^{-5}$  | 0.4–0.9          | 0.24             |
| <i>Model selection: expand</i>  | 500–50,000           | 0.01–1            | 100–31,700         | $10^{-3}$ – $10^{-5}$  | 0.4–0.9          | 1.26             |
| <b>Posteriors</b>               |                      |                   |                    |                        |                  |                  |
| <i>Free model</i>               | 9200 [900–45,600]    | 0.90 [0.26–25.84] | 1100 [100–15,900]  | 5.1e-5 [2.4e-5–1.1e-4] | 0.82 [0.75–0.89] |                  |
| <i>Model selection: expand</i>  | 10,200 [3800–37,900] | 0.47 [0.04–1.00]  | 1900 [1100–19,500] | 4.8e-5 [2.4e-5–9.8e-5] | 0.81 [0.72–0.89] |                  |

ABC analysis of *D. robustus* mtDNA and microsatellite data combined. Priors were incorporated on a log scale with a uniform distribution, but are here shown on a natural scale for clarity.  $N_{cur}$  is 'current' population size, representing effective population size at the last sampling point (602 BP).  $N_{anc}/N_{cur}$  is the size of the 'ancient' effective population size at the onset of demographic change relative to  $N_{cur}$ . Numbers are diploid individuals rounded to the nearest 100; converted from haploids as used in ABCtoolbox.  $T$  is the time at the onset of the demographic change measured in years relative to the youngest sampling point, and rounded to the nearest 100, and converted from generations, as used in ABCtoolbox (generation time assumed to be 10 years for *D. robustus*).  $\mu$  is the microsatellite mutation rate per generation and  $p$  is the shape parameter of the geometric distribution of the General Stepwise Model (see SI text). Marginal densities were compared for the two scenarios in the model selection approach and the Bayes factor support for the *expand* model was 5.25 (1.26/0.24), indicating substantial support (Jeffreys 1961). Posterior parameter estimates represented by mode values and 90% HPDs are shown for the two models with highest marginal density (*free* and *expand* models).